ANIDIS
italian national association for earthquake engineering

PROCEEDINGS OF
THE FRENCH-ITALIAN CONFERENCE
ON

SLOPE STABILITY IN SEISMIC AREAS

May 14-15, 1992
Bordighera (Imperia), Italy

Edited by
E. FACCIOLI
&
A. PECKER

OUEST ÉDITIONS
Presses Académiques

APPLICATION OF THE YIELD DESIGN THEORY TO THE SEISMIC ANALYSIS OF SLOPES

Luc DORMIEUX*, Alain PECKER**, Jean SALENÇON*

Abstract: The present paper describes a method of evaluation of the residual displacements induced by an earthquake in a homogeneous earthdam built in cohesive material. This method constitutes an extension of the yield design theory to the case of a dynamic loading.

Résumé: La présente communication propose une méthode de calcul des déplacements résiduels dus à un séisme dans un barrage homogène constitué d'un matériau purement cohérent. Elle s'appuie sur une extension de la théorie du calcul à la rupture au cas d'une sollicitation dynamique.

1 Introduction

The design of earthdams in earthquake prone areas must account for the inertia forces developing within the soil mass. In the pseudo-static method, this is commonly performed with a classical slope stability analysis in which the static gravity field is modified by introducing horizontal and vertical body forces representing these inertia forces, which are taken constant in time. To overcome these difficulties, the pionnering work of Newmark settled down the idea of a design based on allowable residual (permanent) displacements which the dam undergoes following an earthquake. In the present paper, we propose a method of evaluation of these residual, plane strain, displacements for a homogeneous earthdam built in a purely cohesive material with an undrained shear strength C. This method is related to the one developed by Pecker and Salençon (1991) for the seismic response of shallow foundations.

Under the hypothesis that failure occurs through sliding of a block along a circular surface, the potential failure surface and the critical acceleration, corresponding to the onset of rupture, are determined within the framework of the Yield Design Theory (Salençon, 1983, 1990). Given the acceleration time history at

* Laboratoire de Mécanique des Solides - Ecole Polytechnique - Palaiseau - France

** Géodynamique et Structure - Bagneux, France

the base of the dam, the acceleration field within the earth mass is analytically computed; the residual displacements are then evaluated, for the potentially unstable soil mass, when the computed accelerations exceed the critical threshold.

The method presented herein is not, in essence, different from the one originally proposed by Makdisi and Seed (1979). It however presents, over the latter, the advantages of being analytic and of having a sound mechanical basis within the framework of the Yield Design Theory. Besides, it can be easily implemented on a P.C. and requires only a few seconds to yield the answer; it is therefore easily amenable to parametric studies.

The idea of using the yield design theory for the computations of permanent displacements of a slope submitted to a seismic excitation has already been used by Chang et al (1984). Their work, dedicated to a cohesionless material, is however questionable with regards to the use of the kinematic theorem for a material for which the flow rule is clearly not associated. Besides, the dynamic analysis of the slope, which is reflected by a significant variation of the inertia forces over the volume, is not accounted for in their analysis.

2 Determination of the critical failure surface and computation of the yield acceleration

A schematic drawing of the geometry of the problem under study is given on figure 1.

The acceleration field within the soil mass, whose derivation is given in paragraph 3., is taken parallel to the horizontal direction; furthermore, it is admitted that the inertia forces within a mass $\mathfrak{B}$ can be accounted for in the stability analysis by replacing the actual acceleration field $\underline{a}\ (\underline{x}\ ,\ t)$ by an average field $\underline{\tilde{a}}(t)$ over the mass $\mathfrak{B}$.

$$\underline{\tilde{a}}(t) = \tilde{a}(t)\ \underline{e}_x = \frac{1}{|\mathfrak{B}|} \int_{(\mathfrak{B})} \underline{a}\ (\underline{x}\ ,\ t)\ d\ V \qquad (1)$$

In accordance with the hypothesis of circular shape failure surfaces, the family of blocks represented on figure 2a are analysed. Each block is limited by a circular arc $\widehat{M_1 M_2}$ located in space by the depth of the exit point $h = y\ (M_2)$ and, either by the coordinates of its center Ω, or by the angles θ_1 and θ_2 between the horizontal axis and the vectors $\underline{\Omega M}_1$ and $\underline{\Omega M}_2$. In view of the asymmetry of the structure introduced by the upstream water pressure, only the downstream oriented surfaces are analyzed; situations where the water pressure would have a favorable effect on the stability are excluded. In the same way, for practical purposes, it is sufficient to study situations where the acceleration vector $\underline{a}(t)$ is directed upstream ($\tilde{a} > 0$), so that the inertia body forces $- \rho\, \underline{a}$ are directed downstream. For each block $\mathfrak{B}$, the stability analysis aims at determining the upper limit $\tilde{a}^{cr}_{\mathfrak{B}}$ of $\tilde{a}$, beyond which the equilibrium of the block is no more compatible with the strength of the material.

The yield acceleration $\tilde{a}^{cr}$, associated with the so-called "critical block" $\mathfrak{B}^{cr}$ corresponds to the lowest value of $\tilde{a}^{cr}_{\mathfrak{B}}$:

$$\tilde{a}^{cr} = \inf_{\theta_1,\theta_2,h} \tilde{a}^{cr}_{\mathfrak{B}} (\theta_1,\theta_2,h) \qquad (2)$$

$\tilde{a}^{cr}_{\mathfrak{B}}$ appears to be the threshold of instability related to a circular rupture of block $\mathfrak{B}$ around Ω. It can therefore be determined through the kinematic approach of the yield design theory.

This approach compares the work $W_{ext} (\mathcal{S}, \tilde{a})$, in the failure mechanism, of the external static forces, noted $\mathcal{S}$, and of the inertia forces $- \rho\, \tilde{a}$, to the maximum resisting work W_{res}. The latter represents the maximum energy the soil can set against the failure mechanism, taking into account the material strength capacities.

The kinematic theorem of the yield design theory states that the inequality $W_{ext} (\mathcal{S}, \tilde{a}) \le W_{res}$ is a necessary condition for stability. The threshold of instability $\tilde{a}^{cr}_{\mathfrak{B}}$ is the solution of:

$$W_{ext} (\mathcal{S}, \tilde{a}^{cr}_{\mathfrak{B}}) = W_{res} \qquad (3)$$

with respect to the unknown $\tilde{a}^{cr}_{\mathfrak{B}}$; equation (3) requires the determination of the two quantities W_{ext} and W_{res}. Let $\underline{\hat{\omega}} = \hat{\omega}\, \underline{e}_z$

($\hat{\omega} > 0$) be the virtual rotational velocity of block $\mathcal{B}$ (θ_1, θ_2, h) around Ω, the work of the external forces in such a rigid body motion writes:

$$\mathcal{W}_{ext} (\mathcal{S}, \tilde{a}) = (\underline{\mathfrak{M}}_a + \underline{\mathfrak{M}}_g + \underline{\mathfrak{M}}_w) \cdot \underline{\hat{\omega}} \tag{4}$$

where $\underline{\mathfrak{M}}_a$, $\underline{\mathfrak{M}}_g$, $\underline{\mathfrak{M}}_w$ represent respectively the moments around Ω of the inertia forces, of the gravity forces and of the hydrostatic water pressure.

These moments have a single component along $\underline{e}_z$

$$\underline{\mathfrak{M}}_a = \rho \, \tilde{a} \, X_a \, \underline{e}_z \; ; \; X_a (\theta_1, \theta_2, h) = \int_{(\mathcal{B})} \underline{\Omega M} \cdot \underline{e}_y \, dV \tag{5a}$$

$$\underline{\mathfrak{M}}_g = \rho \, g \, X_g \, \underline{e}_z \; ; \; X_g (\theta_1, \theta_2, h) = \int_{(\mathcal{B})} \underline{\Omega M} \cdot \underline{e}_x \, dV \tag{5b}$$

$$\underline{\mathfrak{M}}_w = \rho_w \, g \, X_w \, \underline{e}_z \; ; \; X_w (\theta_1, \theta_2, h) = \int_{y_W}^{y_{M1}} \underline{\Omega M} \cdot \underline{WM} \, dy \text{ if } y_{M1} > y_W$$

$$X_w = 0 \text{ if } y_{M1} \leq y_W \tag{5c}$$

where W represents the intersection of the upstream slope with the free surface of the reservoir (figure 1).

The resisting work in the rotational movement of $\mathcal{B}$ arises from the velocity discontinuity $[\![\underline{v}]\!]$ along the arc $\widehat{M_1M_2}$. Since the discontinuity is tangent to the arc $\widehat{M_1M_2}$, it is associated with a resisting work per unit length equal to $C|[\![\underline{v}]\!]|$ whose integral is $\mathcal{W}_{res}$:

$$\mathcal{W}_{res} = \int_{\widehat{M_1M_2}} C|[\![\underline{v}]\!]| \, d\ell = C R^2 (\theta_2 - \theta_1) \hat{\omega} \tag{6}$$

where R is the radius of the arc $\widehat{M_1M_2}$. Using (4) and (6), the inequality of the kinematic theorem writes:

$$\rho\, \tilde{a}\, X_a + \rho\, g\, X_g + \rho_w\, g\, X_w \leq C\, R^2\, (\theta_2 - \theta_1) \tag{7}$$

According to (3), the threshold of instability $\tilde{a}^{cr}_{\mathcal{B}}$ for the set of parameters θ_1, θ_2, h is obtained for the equality in equation (7).

Whenever the 3-parameters set (θ_1, θ_2, h) takes all the permissible values, the set of inequalities (7) defines a family of necessary conditions for stability. As anticipated, the systematic numerical evaluation indicates that the most stringent stability condition is achieved, h being given, when the inertia forces, the gravity force and the water pressure are all driving forces (X_a, X_g, $X_w \geq 0$). The yield acceleration $\tilde{a}^{cr}$ is then given by (2):

$$\tilde{a}^{cr} = \inf_{\theta_1, \theta_2, h} \left\{ \frac{C\, R^2\, (\theta_2 - \theta_1)}{\rho\, X_a} - g \left(\frac{X_g}{X_a} + \frac{\rho_w}{\rho}\, \frac{X_w}{X_a} \right) \right\} \tag{8}$$

excluding from the search the sets of parameters (θ_1, θ_2, h) for which $X_a \leq 0$. It turns out that the yield acceleration is reached when the exit point of the failure surface is at the downstream toe of the dam (h = H).

In aseismic conditions, i.e. $\tilde{a} = 0$, we define a confidence factor with respect to a circular failure along the arc $\widehat{M_1 M_2}$ as the ratio, when the inertia forces and gravity forces are driving forces $(\rho\, g\, X_g + \rho_w\, g\, X_w > 0)$:

$$F\, (\theta_1, \theta_2, h) = \frac{C\, R^2\, (\theta_2 - \theta_1)}{\rho\, g\, X_g + \rho_w\, g\, X_w} \tag{9}$$

With this definition, (8) can be written:

$$\frac{\tilde{a}^{cr}}{g} = \inf_{\theta_1, \theta_2, h} \left\{ \left[\frac{X_g\, (\theta_1, \theta_2, h)}{X_a\, (\theta_1, \theta_2, h)} + \frac{\rho_w}{\rho} \cdot \frac{X_w\, (\theta_1, \theta_2, h)}{X_a\, (\theta_1, \theta_2, h)} \right] \cdot \left(F\, (\theta_1, \theta_2, h) - 1 \right) \right\} \tag{10}$$

For a stable structure in aseismic conditions, the confidence factor F (θ_1,θ_2,h) is greater or equal to 1 and $\tilde{a}^{cr}$ is therefore a positive or nul scalar quantity. The 3-parameters set (θ_1,θ_2,h) associated with the minimum of (10) defines the critical block $\mathfrak{B}^{cr}$ and the corresponding potential failure surface.

3 Computation of the acceleration field

The computations are based on the shear beam model originally developed by Ambraseys (1960) and Ambraseys-Sarma (1967). It has been extensively used to estimate the lateral seismic response of earthdams, its popularity stemming mainly from its simplicity. A number of rigorous studies have largely corroborated one of the crucial assumptions of the shear beam model, i.e. that strains and displacements are uniformly distributed over the width of the dam.

In the present paper, we restrict our attention to a homogeneous dam with uniform properties (modulus and mass density) over height. More realistic assumptions regarding the variations of the shear modulus G have been studied by Dakoulas and Gazetas (1985) and could be implemented without further difficulties.

Referring to figure 3, the governing equation of motion is derived by considering the dynamic equilibrium of an infinitesimal slice of thickness dy and width b.

$$\rho \frac{\partial^2 \underline{u}^*}{\partial t^2} = \frac{1}{y} \frac{\partial}{\partial y} \left[y\, G \frac{\partial \underline{u}}{\partial y} \right] \qquad (11)$$

where:

$\underline{u}$ horizontal relative displacement with respect to base,

$\underline{u}^*$ absolute displacement = $\underline{u} + u_g \underline{e}_x$

u_g displacement of the base

G shear modulus

Introducing the shear wave velocity ($\rho V_s^2 = G$), (11) can be written

$$\frac{\partial^2 \underline{u}}{\partial y^2} + \frac{1}{y} \frac{\partial \underline{u}}{\partial y} - \frac{1}{V_s^2} \frac{\partial^2 \underline{u}}{\partial t^2} = \frac{1}{V_s^2} \frac{d^2 u_g}{d t^2} \underline{e}_x \qquad (12)$$

Equation (12) is solved using modal superposition; hence $\underline{u}(y,t)$ is obtained as a summation of discretely infinite number of displacement histories corresponding to each of the natural frequencies of the dam

$$\underline{u}(y,t) = \left(\sum_{n=1}^{\infty} P_n U_n(y) D_n(t) \right) \underline{e}_x \tag{13}$$

where $D_n(t)$ is the well-known Duhamel integral.

The absolute acceleration is given by:

$$\underline{a}(y,t) = \underline{e}_x \left[\sum_{n=1}^{\infty} P_n U_n(y) D''_n(t) \right] + \ddot{u}_g \left[1 - \sum_{n=1}^{\infty} P_n U_n(y) \right] \underline{e}_x \tag{14}$$

with

$$I_n = \omega_n \int_0^t \ddot{u}_g(\tau) e^{-\beta\omega_n(t-\tau)} \sin[\omega_n^* (t-\tau)] \, d\tau$$

$$J_n = \omega_n \int_0^t \ddot{u}_g(\tau) e^{-\beta\omega_n(t-\tau)} \cos[\omega_n^* (t-\tau)] \, d\tau$$

$$D''_n(t) = \frac{d^2}{dt^2} D_n(t) = \frac{1 - 2\beta^2}{(1 - \beta^2)^{1/2}} I_n + 2 \beta J_n \tag{15}$$

$$P_n = \frac{2}{q_n} \frac{1}{J_1(q_n)} \tag{16a}$$

$$U_n(y) = J_0 \left(q_n \frac{y}{H} \right) \tag{16b}$$

where q_n is the n^{th} root of $J_0(.) = 0$; J_0 and J_1 are Bessel's functions of order 0 and 1; β is the material damping ratio.

ω_n is the undamped circular frequency $= q_n \frac{V_s}{H}$ and ω_n^* the damped circular frequency.

A realistic evaluation of the acceleration field $\underline{a}$ (y,t) usually requires that at least 10 modes be included in the analysis.

Referring to figure 4, the average acceleration $\tilde{a}(t)$ over a given depth is then computed as the acceleration developing the same inertia forces within the potentially sliding block (eq. 1). Considering the simplified geometry of figure 4, which is a valid approximation for a circular arc, it can readily be shown that:

$$\tilde{a}\,(t) \;=\; \frac{2}{Y^2} \int_0^Y a\,(y,t)\; y\; dy \tag{17}$$

A further refinement is introduced in the computations by computing the strain compatible properties for the dike. Following Makdisi and Seed (1979), the average shear strain through the dam is computed as, retaining only the first mode:

$$(\gamma_{av}) \;\simeq\; 0.2\;\frac{H}{V_s^2}\;\underset{t}{\mathrm{Max}}\;[D_1''\,(t)] \tag{18}$$

from which the compatible damping ratio β and shear modulus G (or shear wave velocity V_s) can be evaluated. A few iterations are required to achieve convergence and $\tilde{a}$ (t) can then be computed from (14) to (17) with the appropriate value of V_s and β.

4 Evaluation of the permanent displacements

In the preceding paragraph, the time history of the average acceleration $\tilde{a}$ (t) has been derived for any potentially unstable block. At the critical time t^{cr} when $\tilde{a}(t)$ reaches the yield acceleration $\tilde{a}^{cr}$, a rupture along the arc $\widehat{M_1M_2}$ is initiated (figure 5). The evaluation of the permanent, irrecoverable, displacements taking place from that time is based on two hypotheses: the first one deals with the kinematic of the rupture and the second one has to do with the material behavior.

Let (Ω, $\underline{e}_x$, $\underline{e}_y$, $\underline{e}_z$) be the coordinates axes attached to the dam, translated with respect to a fixed reference according to the acceleration time history $\tilde{a}$ (t). It is assumed that, beyond the critical time t^{cr}, the kinematic of the block $\mathfrak{B}^{cr}$, relative to the reference $(\Omega, \underline{e}_x, \underline{e}_y, \underline{e}_z)$ is a rigid body rotation around the axis Ω_z, whose angular velocity is noted $\underline{\omega}(t) = \omega(t)\, \underline{e}_z$. The circular arc $\widehat{M_1M_2}$ along which sliding takes place, is a surface of discontinuity for the velocity field within the dike. In compliance with an elastoplastic constitutive behavior, the second hypothesis states that, as soon as sliding occurs, the stress state along the failure surface is located on the boundary of the elastic domain of the material, defined by (3). In other words, equality is ensured in (3) if $\omega \neq 0$

$$\omega > 0 \quad \Rightarrow \quad \tau = C \tag{19a}$$

$$\omega < 0 \quad \Rightarrow \quad \tau = -C \tag{19b}$$

To compute the time history of motion, i.e. $\omega(t)$, it is convenient to apply the principle of virtual work. It implies that, in a Galilean referential, for any rigid body, virtual motion $\underline{\hat{u}}$ of the block $\mathfrak{B}^{cr}$, the work $\mathfrak{A}(\underline{\hat{u}})$ of the acceleration momentum is equal to the work of the external forces acting on the block. The principle of virtual work is now applied to the rotational velocity field in the relative motion of $\mathfrak{B}^{cr}$ with reference to the dike which is taken as a particular virtual motion.

The absolute acceleration $\underline{\gamma}(t)$ of block $\mathfrak{B}^{cr}$ writes down:

$$\underline{\gamma}(t) = \underline{\tilde{a}}(t) + \underline{\omega} \wedge (\underline{\omega} \wedge \underline{\Omega M}) + \underline{\dot{\omega}} \wedge \underline{\Omega M} \tag{20}$$

and the work of the acceleration momentum $\rho\, \underline{\gamma}$ in the relative motion $\underline{U}^r$ is given by:

$$\mathfrak{A}(\underline{U}^r) = \underline{\omega} \,.\, \int_{(\mathfrak{B}^{cr})} (\underline{\Omega M} \wedge \rho\, \underline{\tilde{a}})\, dV + \int_{(\mathfrak{B}^{cr})} (\rho\, [\underline{\omega} \wedge \underline{\Omega M}].[\underline{\dot{\omega}} \wedge \underline{\Omega M}])dV \tag{21}$$

or

$$\mathfrak{A}(\underline{U}^r) = \omega(t)\, (J\, \dot{\omega}(t) - \rho\, \tilde{a}(t)\, X_a) \tag{22}$$

where J is the mass moment of inertia of block $\mathfrak{B}^{cr}$ around the axis Ω_z.

The work of the gravity forces, of the water pressure and of the contact forces along the arc $\widehat{M_1M_2}$ in the relative rotational motion of block $\mathfrak{B}^{cr}$ is equal to the scalar product: $\underline{\omega}$ (t) . ($\underline{\mathfrak{M}}_g$ + $\underline{\mathfrak{M}}_w$ + $\underline{\mathfrak{M}}_\sigma$).

Finally, the principle of virtual work yields the following equality:

$$J \dot{\omega} (t) = \rho \tilde{a} (t) X_a + \rho g X_g + \rho_w g X_w - R \int_{\widehat{M_1M_2}} \tau (t) \, d \ell \qquad (23)$$

or, from equation (8):

$$J \dot{\omega} (t) = \rho X_a (\tilde{a}(t) - \tilde{a}^{cr}) + C R^2 (\theta_2 - \theta_1) - R \int_{\widehat{M_1M_2}} \tau (t) \, d\ell \qquad (24)$$

The situation $\omega < 0$ would correspond to an upstream ("up the slope") movement of the block, in which the gravity forces and the upstream water pressure would be resisting forces. Although that situation could be treated without any additional difficulty, it is not considered in the following and the angular velocity is consequently greater or equal to 0. Introducing (19a) in (24), it follows that:

$$\omega > 0 \Rightarrow J \dot{\omega} (t) = \rho X_a (\tilde{a} (t) - \tilde{a}^{cr}) \qquad (25)$$

According to the sign of $(\tilde{a} (t) - \tilde{a}^{cr})$, the block movement is either accelerated or decelerated. If $\omega = 0$, the result depends on the value of $\tilde{a}$ (t).

$$\omega = 0: \quad \begin{cases} \text{if } \tilde{a}(t) \geq a^{cr}, \ J \dot{\omega} (t) = \rho X_a(\tilde{a}(t) - \tilde{a}^{cr}) \\ \text{if } \tilde{a}(t) < a^{cr}, \ \dot{\omega} (t) = 0 \end{cases} \qquad (26)$$

Equations (25) and (26) are used to numerically integrate the time history of motion (24) with a time discretization of the input motion.

5 Examples

An interesting question to answer is: given a sufficiently conservative static design of the dam (with respect to the two loading parameters: the dead load and the upstream water pressure), is it possible to prevent excessive seismic permanent displacements from occurring? The results presented hereafter throw some light on this question although without bringing a definite answer.

The idea consists in plotting the horizontal displacement of point A (figure 1) as a function of the static confidence factor F. More precisely, given the geometry of the dike and the static loads, the confidence factor is varied by altering the undrained shear strength of the material. For a given seismic input motion, the maximum amplitude of the horizontal displacement $\xi_x(A)$ is computed for each shear strength value. The variations of $\xi_x(A)$, as a function of F, are given on figure 6 for the data gathered in table I. The seismic input motion is the N21E component of the Kern County California earthquake of July 1952 (magnitude M = 7.6), recorded at Taft and scaled to a maximum acceleration of 0.3 g (duration 30 s).

Geometry	Material properties
$H = 45$ m $d = 10$ m $\alpha = 20°$ $h_w = 45$ m	$V_s = 285\ m.s^{-1}$ $\beta = 0.2$ $\gamma_r = 3\ 10^{-4}$

TABLE I

The graph exhibits a hyperbolic shape which could be anticipated. The displacements take large values, associated with an almost complete failure of the dam, when F tends to 1. On the other hand, the displacements are equal to zero for a confidence factor above 1.7 and do not exceed 5 cm when the confidence factor is larger than 1.5. Care must however be taken not to generalize these results to other geometries.

Figure 7 gives the variation of the horizontal displacement at point A versus the water height in the reservoir. The displacement amplitude is insensitive to the water height as long as the latter remains smaller than 2/3 of the total dam height; it then increases to reach a value equal to 3 times the initial value. The existence of this threshold can be explained by looking at the geometry of the critical block $\mathcal{B}^{cr}$: for sufficiently low water levels in the reservoir, the location of the exit point M_1 of the potentially unstable block is located above the reservoir free surface so that the water pressure does not contribute to the motion.

References

N.N. Ambraseys (1960). On the shear response of a two dimensional truncated wedge subjected to an arbitrary disturbance. *Bulletin of Seismological Society of America*, 50, n° 45.

N.N. Ambraseys, S.K. Sarma (1967). The response of earthdams to strong earthquakes. *Geotechnique* n° 17, (3).

C.J. Chang, W.F. Chen, J.T.P. Yao (1984). Seismic displacements in slopes by limit analysis. *Geotech. Eng. Division, ASCE*, 110, GT7.

P. Dakoulas, G. Gazetas (1985). A class of inhomogeneous shear models for seismic response of dams and embankments. *Soil Dynamics and Earthquake Engineering*, 4, n° 4.

A.M. Makdisi, H.B. Seed (1979). Simplified procedure for evaluating embankment response. *J. Geotech. Eng. Division - ASCE* 105, GT12.

A. Pecker, J. Salençon (1991). *Seismic bearing capacity of shallow strip foundations on clay soils*. CEE Mexico International Workshop.

J. Salençon (1983). *Calcul à la rupture et analyse limite*. Presses de l'Ecole Nationale des Ponts et Chaussées.

J. Salençon (1990). An introduction to the yield design theory and its application to soil mechanics. *European Journal of Mechanics, A/Solids*, 9, n° 5.

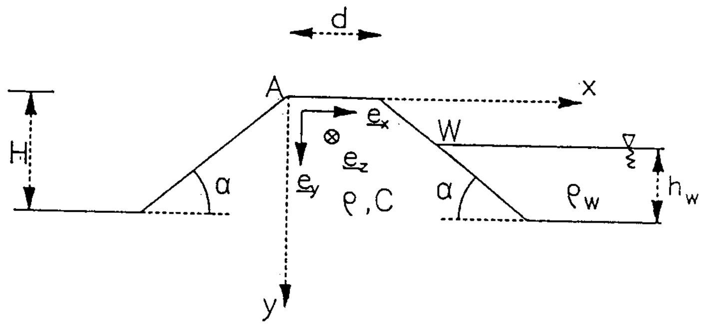

Fig. 1: Geometry and notations

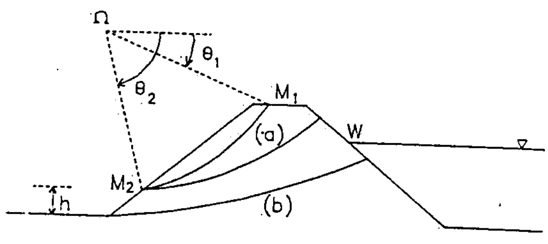

Fig. 2a: The different components of loading

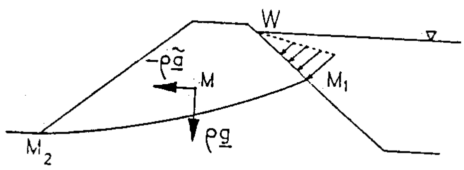

Fig. 2b: Circular failure surfaces

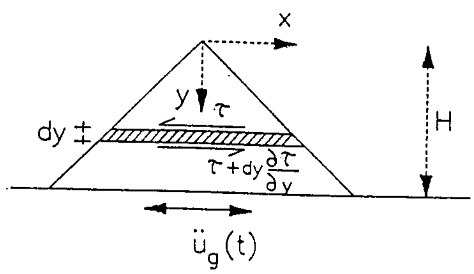

Fig. 3: Dam cross section – Shear beam model

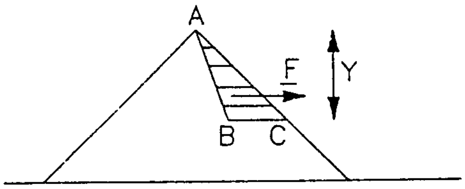

$$\underline{F} = \rho\, \tilde{\underline{a}}(t)\, V_{ABC} = \int_{[ABC]} \rho \underline{a}(y,t)\, dV$$

Fig. 4: Computation of average accelerations

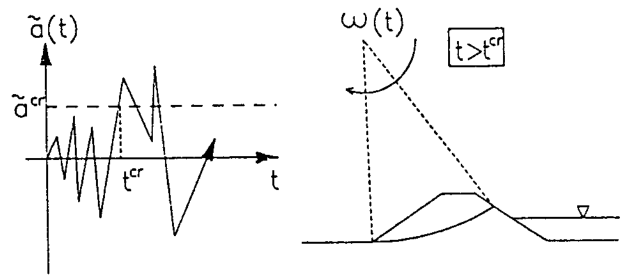

Fig. 5: Beginning of sliding

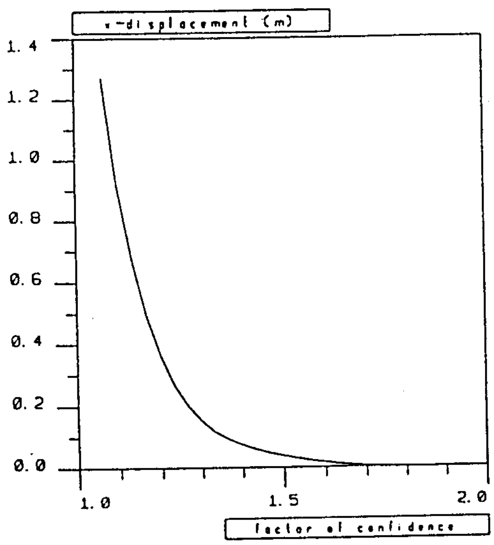

Fig. 6: Variation of ξ_x (A) with the static factor of confidence

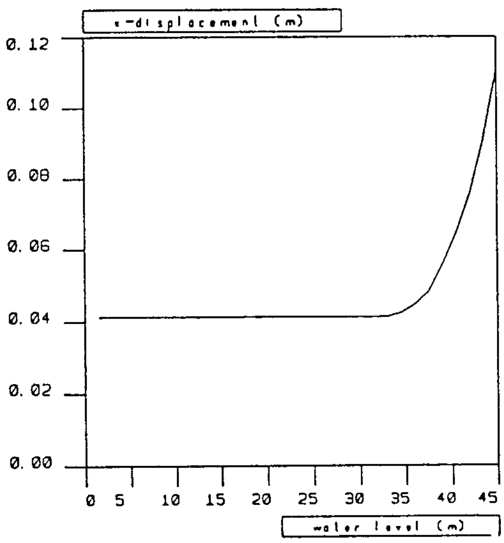

Fig. 7: Variation of ξ_x (A) with the water level in the reservoir